arXiv:2205.09747v1 [cs.RO] 19 May 2022

HandoverSim: A Simulation Framework and Benchmark for Human-to-Robot Object Handovers

Yu-Wei Chao[1], Chris Paxton[1], Yu Xiang[2], Wei Yang[1], Balakumar Sundaralingam[1], Tao Chen[3], Adithyavairavan Murali[1], Maya Cakmak[1,4], Dieter Fox[1,4]

***Abstract*— We introduce a new simulation benchmark "HandoverSim" for human-to-robot object handovers. To simulate the giver's motion, we leverage a recent motion capture dataset of hand grasping of objects. We create training and evaluation environments for the receiver with standardized protocols and metrics. We analyze the performance of a set of baselines and show a correlation with a real-world evaluation.** [1]

I. Introduction

The ability to exchange objects with humans seamlessly and safely is crucial for human-robot interaction (HRI). Progress on this front can impact robots across many application domains including domestic robots, assistive robots for older adults and people with disabilities, and collaborative robots in manufacturing.

Despite increasing efforts [1], current research on human-robot object handovers still faces two key challenges. First, evaluation often requires a real human in the loop. This makes the evaluation process expensive and harder to reproduce. Second, different studies often adopt different experimental settings (e.g., objects used) and evaluate with different metrics. This makes cross-study comparison difficult.

Standardized datasets and benchmarks have played a key role for recent progress in computer vision and machine learning [2], [3]. In robotics, there has also been increasing efforts in improving reproducibility through standardized benchmarks with simulation [4], [5], [6], [7], [8], [9], [10], [11], [12], [13], [14]. This has impacted various domains from object manipulation [4], [6], navigation [5], [7], to even assisting humans [9], [10]. Our work extends these efforts to the critical HRI problem of object handovers.

Building a simulation-based benchmark for human-robot object handovers is uniquely challenging. A key question is how we can simulate a realistic human agent and its interaction with the robot during a handover process. Photo and physics realistic simulation of humans has been widely studied in graphics but still under active research. Furthermore, object handovers involve contact-rich interactions between human hands and objects. A high fidelity simulation requires substantial physics modeling and sophisticated simulation capabilities on soft body dynamics.

In this work, we introduce HandoverSim: a new simulation framework and benchmark for human-to-robot object handovers. We focus on the less explored but challenging human-to-robot (H2R) paradigm [1], where the robot has to take over an object handed over by a human. As the first step, we focus specifically on the realism of hand motion in simulating the human giver. We leverage a recent motion capture dataset of human grasping objects and performing handover attempts [15], and build a simulation environment where the motion of the human giver is driven by the captured motion. Overall, the environment contains 1,000 handover scenes captured from 10 subjects handing over 20 different objects in the real world. Based on this environment, we create a new benchmark for training and evaluating robots on H2R object handovers.

Our contributions are threefold. First, we propose a new framework for simulating the giver's motion in H2R handovers. Second, we introduce a new benchmark environment which enables standardized and reproducible evaluation of receiver policies. To the best of our knowledge, this is the first simulation benchmark for H2R handovers. Finally, we analyze the performance of a set of baselines, including a motion planning method, a task planning method, and a pre-trained reinforcement learning policy. We further show a positive correlation between the performance achieved on our benchmark and a real-world user study.

II. Related Work

Object Handovers. Human-robot handovers has been increasingly studied over the past decade [1], achieving impressive progress on different robot capabilities including intent communication [16], grasp planning [17], perception [18], [19], handover location selection [20], [21], motion planning and control [22], grip force modulation [23] and error handling [24]. However, previous works diverge on experimental settings and metrics, making fair comparisons difficult. Our HandoverSim evaluates H2R handovers in a physics simulated environment with a broad set of objects and a unified set of evaluation metrics commonly used in handover research. Its introduction can facilitate easy and fair comparison among different handover approaches.

Simulation for Robotics. Simulation environments have been increasingly used in robotics since they enable scalable training of robots and standardized evaluation. Some environments focus specifically on simulating large-scale indoor scenes [25], [26], [27], [28], [29], [30], [5], [12]. They are typically used for navigation related tasks and are often lacking on interactability and physics realism. Some others focus on object manipulation and thus require a

[1]NVIDIA, [2]UT Dallas, [3]MIT CSAIL, [4]University of Washington
@{ychao,cpaxton,weiy,balakumars,admurali,mayacakmak,dieterf}@nvidia.com
@yu.xiang@utdallas.edu @taochen@mit.edu

[1]Code is open sourced at https://handover-sim.github.io.

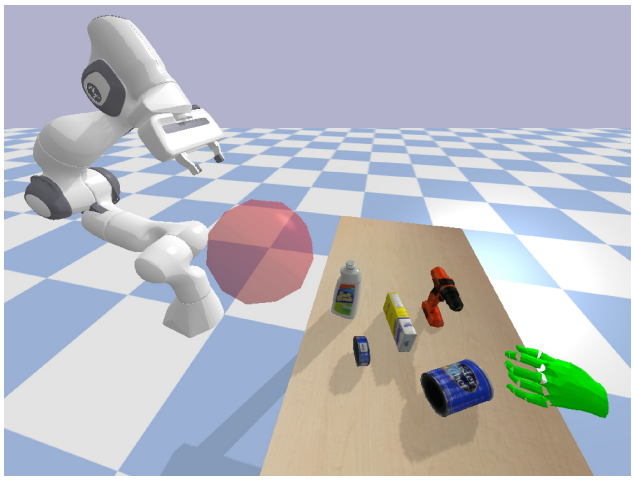


Fig. 1: Our simulation environment for human-to-robot object handovers. Green: human hand. Red sphere: goal region.

high fidelity physics simulation for realistic interactions [4], [6], [8], [7], [11], [13], [31]. Nonetheless, neither of these environments contain simulated humans. Most related to ours are the recently introduced Assistive Gym [10] and Watch-and-Help [32], both contain human-like agents in simulation. Assistive Gym [10] is a physics simulated environment for training robots to assist people with activities of daily living. While they simulate robot-human physical interactions, their virtual humans are either completely passive or driven by motion trained with a cost function. In contrast, we drive our simulated human hands with motion captured from real humans. Watch-and-Help [32] is an environment based on VirtualHome [33] for evaluating social intelligence. They focus primarily on high-level task learning and thus do not simulate realistic physical interactions.

Handover Benchmarks. Our work is also related to recent efforts on standardizing the experimental setting and protocol for handovers. Ye et al. [34] proposed a large-scale human-to-human handover dataset with object and hand pose annotations, and used it to study human grasp prediction. Rather than predicting human grasps, Chao et al. [15] studied robot grasp generation for safe H2R handovers. While these works promote a fair benchmark for handover research, their tasks are formulated only at the vision level, without any physics simulated evaluation. Sanchez-Matilla et al. [35] proposed a real-world benchmark for H2R handovers of unseen cups with unknown filling. However, they only considered objects of a single category, i.e., cups. Our HandoverSim contains the commonly used YCB objects [36] and allows a physics simulated evaluation of the full handover process.

III. Simulating Handovers

We assume the scene contains a human giver and a robot arm receiver facing each other with a table in between, and a set of objects initially placed on the table, as shown in Fig. 1. The human giver will pick up an object from the table with a single hand (right or left) and offer it to the robot. The robot receiver is able to observe the human's actions and the scene, and react simultaneously to eventually take over the object from the human's hand.

To simulate the physical interaction of this process, we build a simulation environment using the PyBullet physics engine [37]. [2] For the choice of the robot, we use a model of the commercial Franka Emika Panda with a 7-DoF arm and a 2-DoF parallel-jaw gripper. While the described handover process is a two-agent game (between the human and robot), in the benchmark we expect the robot to be the only controllable agent and can move freely within its own physical limits. A key question is then how we can simulate a realistic human giver, particularly on their motion and interaction with the robot. Below we describe our approach.

Grasping and Offering Object. To simulate realistic human motion of object grasping and offering, we leverage a recent human grasping dataset called DexYCB [15]. DexYCB captures real motion of human subjects picking up an object from a table of objects, and handing it to an imagined partner across the table. A typical capture starts from the subject in a relaxed pose, and ends in the subject's hand holding the object in the air, waiting for a receiver to acquire it. Each capture provides frame-wise 3D pose of both the hand in use and the objects in the scene. This data serves as an ideal basis for the human giver's motion in the "pre-handover" phase [1] (i.e., before the receiver's hand contacting the object). We therefore use these captures to drive the human giver's motion in simulation.

We first import object and hand models into simulation. DexYCB uses 20 objects from the YCB-Video dataset [36], where object pose is represented by the 6D pose of a rigid mesh. Hand pose is represented by the deformable MANO mesh model [39], parameterized by two low-dimensional embeddings for shape and articulation. We use [40] to import MANO into PyBullet, which turns the hand into an articulated rigid body after the shape deformation.

One approach to reproducing the captured motion in simulation is to learn a control policy to actuate the human hand to pick up the object with close fidelity to their captured trajectories [41]. However, learning to control a dexterous hand to manipulate objects has been notoriously challenging [42], [43], [44] and requires a significant engineering effort on the hand's physics model. Hence we take a different approach: rather than relying on the human hand to physically move the object, we augment the object models by adding additional actuators to their base such that their 6D pose can be directly actuated by controllers in simulation. Consequently, we can directly control the human hand and the grasped object to simultaneously move according to their captured trajectories. Due to the noise in motion capture, the data may contain moderate interpenetration between the hand and object model during grasping. We thus disable the collision detection between the human hand and object to avoid artifacts caused by unstable simulation. For each capture, we simulate a handover trial by "replaying" the motion from the first frame. After reaching the last frame, we force the hand and object

[2] Support of Isaac Gym [38] has been added upon publication of the paper.

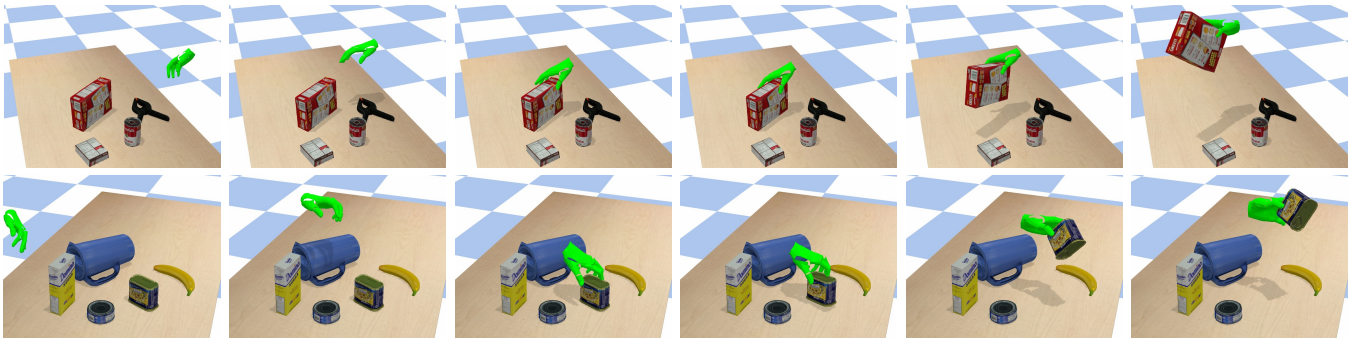


Fig. 2: Simulated human hand and object motion for handovers. Top: right hand. Bottom: left hand.

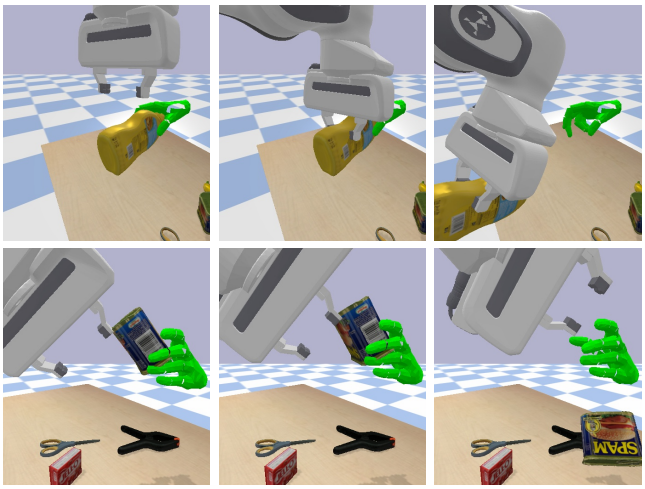


Fig. 3: Simulating objects released from human hands. A release is triggered at the middle frame in the top and bottom examples.

to stay in the end pose, i.e., simulating the giver waiting still for the receiver. Fig. 2 shows two examples of the simulated human hand and object motion.

Releasing Object. Once we can simulate a human presenting an object for handover, the next question to simulate the release of the object to the robot, i.e., the "physical handover" phase [1]. Since the object's pose has so far been actively controlled, we need to disable the controller to simulate a release. We simulate releases in two scenarios. An "active" release (i.e., a voluntary release from human) is triggered when the object has been in contact with both gripper finger's gripping surface continuously for 0.1 seconds. In addition to releasing voluntarily, the object can also drop involuntarily, e.g., due to robot arm strikes. Therefore, we also trigger a "passive" (i.e., compulsive) release when the object has been free of contact with either gripping surface but has been in contact with any other parts of the robot body continuously for 0.1 seconds. Once triggered, the object becomes completely passive and is only subject to robot forces and gravity. Fig. 3 shows two examples of the triggered release.

Remarks. We make two remarks regarding our simulation of the human giver: (1) Our human's motion is non-adaptive to the robot's actions. This assumption is rather naive but still applies in many human-robot collaboration scenarios where the human is cognitively engaged in some other tasks and has to exchange objects with robots "blindly". (2) We do not simulate realistic human hand motion during object release and post-release due to the lack of such data.

IV. Benchmark Environment

Using the proposed simulation framework, we construct a new benchmark environment called HandoverSim.

Task. We formalize the task as standard reinforcement learning (RL) problems and implement the benchmark environment using the OpenAI Gym API [45]. At each time step t, the robot agent observes the current state of the environment $s_t \in \mathcal{S}$, and has to generate an action $a_t \in \mathcal{A}$ from its policy. The action a_t is then executed in the environment, which returns a new state s_{t+1} and optionally a scalar reward r if an RL algorithm is used. $\mathcal{A}$ is a 9-dimensional continuous space where an action specifies the target joint position for a PD controller of the robot arm (7 DoF) and gripper (2 DoF). $\mathcal{S}$ may vary depending on the benchmark setting, e.g., object pose or point cloud.

For quantitative evaluation we need to programmatically define when a task is succeeded or failed. We claim that a *success* is achieved when the below three conditions are met:

1) The gripper fingers are in contact with the handed over object.
2) The position of the gripper link lies with a pre-specified goal region (Fig. 1).
3) The above two conditions hold true continuously for 0.1 seconds.

We establish a spherical goal region (Fig. 1) in close proximity in front of the robot arm to prevent a success case where the robot has reached the object but got stuck due to an unnatural pose configuration. The robot instead should be able to pull back the object to close proximity after taking hold of it and potentially use it to perform other tasks. On the other hand, a *failure* is detected when either one of the following three conditions is met:

1) Any part of the robot body is in contact with any part of the human hand.
2) At least one of the gripper fingers is not in contact with the handed over object and the object is in contact with the table or other objects or its center falls below the height of the table surface.

	S0: default				S1: unseen subjects				S2: unseen handedness				S3: unseen grasping			
	#sub	hand	#obj	#sce	#sub	hand	#obj	#sce	#sub	hand	#obj	#sce	#sub	hand	#obj	#sce
train	10	R/L	18	720	7	R/L	18	630	10	R	18	449	10	R/L	14	700
val	2	R/L	18	36	1	R/L	18	90	2	L	18	91	10	R/L	2	100
test	8	R/L	18	144	2	R/L	18	180	8	L	18	360	10	R/L	2	100
all	10	R/L	18	900	10	R/L	18	900	10	R/L	18	900	10	R/L	18	900
all*	10	R/L	20	1,000	10	R/L	20	1,000	10	R/L	20	1,000	10	R/L	20	1,000

TABLE I: Statistics of the four evaluation setups: S0, S1, S2, and S3. For each setup, we list the number of subjects (#sub), hands used (right: R, left: L, or both: R/L), number of objects (#obj), and number of scenes (#sce). "all*" includes all the sequences from DexYCB, and "all" is after removing objects ungraspable by the gripper.

3) A maximum time limit of 13 seconds has reached.

The first condition (referred to as "contact") prohibits robot-human contacts to avoid potential harms to human (e.g., human hand pinched by the gripper) and ensures a safe handover process. The second condition (referred to as "drop") prohibits the robot from dropping the object. The third condition (referred to as "timeout") ensures that the task is completed within a reasonable time length.

Evaluation Metrics. Object handover is commonly regarded as a multi-objective task in HRI [1]. For our benchmark, we report metrics on *efficacy*, *efficiency* and *safety*. First, using the definitions of success and failure mentioned above, we terminate an episode whenever a success or failure is detected. This way an episode can only belong to a success or failure case, but not both, i.e., we do not allow the robot to complete the task after touching the human hand. To evaluate efficacy, we calculate the success rate over all the test episodes, and also the failure rate from each of the three failure causes: "contact", "drop", and "timeout". For efficiency, we calculate the mean completion time over the successful episodes. Note that we do not include episodes of failure in this metric. We further divide the completion time into execution time and planning time. The execution time ("exec") is the accumulated time during which the robot is physically moving, and depends only on the number of time steps in an episode. The planning time ("plan") is the accumulated wall time on running the policy function. Finally, we regard the failure rate due to robot-human contacts (i.e., "contact") as our safety metric.

Environment Statistics. DexYCB [15] captures 10 subjects grasping 20 objects with 5 trials per subject-object pair. This amounts to 1,000 motion capture sequences where each sequence captures a single trial. We adopt all the sequences and simulate one handover scene from each sequence, resulting in 1,000 *scenes*. Among the 5 trials, the first two use the right hand, the next two use the left hand, and the choice of the last one is randomized. This results in approximately an equal number of handover attempts from both the right and left hand. The object to be grasped is initially placed on the table and mixed with 2 to 4 other objects in randomized pose configuration. Each sequence (for simulating the "pre-handover" phase) is slightly less than 3 seconds, containing the full course of action from pickup to offering for handover.

Training and Evaluation Setup. We expect the benchmark to be used not only for evaluation but also for training. Therefore, we divide the scenes into train/val/test splits following standard machine learning paradigms. Due to limitations in gripper capacity, we first remove scenes where the robot has to grasp the following two objects: "002_master_chef_can" and "036_wood_block". Next, following DexYCB [15], we generate four different *setups* by splitting the scenes in four different ways to benchmark different scenarios:

- **S0 (default).** The train split contains all 10 subjects and all 18 grasped objects.
- **S1 (unseen subjects).** The scenes are split by subjects (train/val/test: 7/1/2).
- **S2 (unseen handedness).** The scenes are split by handedness, i.e., right or left hand used (train/val/test: R/L/L).
- **S3 (unseen grasping).** The scenes are split by the grasped objects (train/val/test: 14/2/2).

Tab. I shows the statistics of the four setups. For evaluation, each policy is ran for one single episode in each test scene.

V. Experiments

We select a set of baselines and studied their performance on HandoverSim. As the first benchmark, we study a simple setting where we assume the ground-truth states of the human hand and objects (retrieved from simulation) are available to the policy, i.e., we assume a perfect perception and focus the evaluation solely on planning and control capabilities. For a fair comparison of planning time, all the baselines are ran on the same platform with an AMD Ryzen 9 5950X CPU with 128 GB RAM and an NVIDIA GeForce RTX 3090 GPU.

Baselines. Our baselines are adopted from three prior works:

- **OMG Planner [46].** This is a joint motion and grasp planner. It takes in the robot's current configuration and a set of candidate goal configurations, and jointly selects a goal and generates a trajectory towards it based on trajectory optimization. Since this is an open loop planner, we force the robot to stay in the start pose while the human hand is moving. Once the human hand reaches the end pose and begins the wait, we then use the object's pose for planning. To obtain the goal set, the planner uses pre-generated grasp poses for each YCB object from [47]. Once the robot traverses to the end of the planned trajectory, we switch to a hand coded policy that closes the gripper and moves towards the handover goal region. Note that this baseline does not take the human hand into account.
- **Yang et al. [17].** This is a reactive H2R handover system which performs point cloud-based grasp generation followed by task planning for grasp selection. Since we

	S0: default							S1: unseen subjects						
	success	mean accum time (s)			failure (%)			success	mean accum time (s)			failure (%)		
	(%)	exec	plan	total	contact	drop	timeout	(%)	exec	plan	total	contact	drop	timeout
OMG Planner [46]	62.50	8.309	1.414	9.722	27.78	**8.33**	**1.39**	**62.78**	8.012	1.355	9.366	33.33	**2.22**	**1.67**
Yang et al. [17]	**64.58**	4.864	**0.036**	4.900	17.36	11.81	6.25	**62.78**	4.719	**0.039**	4.758	14.44	7.78	15.00
GA-DDPG [48] hold	50.00	7.139	0.142	7.281	**4.86**	19.44	25.69	55.00	6.791	0.136	6.927	**8.89**	15.00	21.11
GA-DDPG [48] w/o hold	36.81	**4.664**	0.132	**4.796**	9.03	25.00	29.17	33.33	**4.261**	0.132	**4.393**	15.56	21.67	29.44
	S2: unseen handedness							S3: unseen grasping						
	success	mean accum time (s)			failure (%)			success	mean accum time (s)			failure (%)		
	(%)	exec	plan	total	contact	drop	timeout	(%)	exec	plan	total	contact	drop	timeout
OMG Planner [46]	**62.78**	8.275	1.481	9.755	30.56	**3.89**	**2.78**	**69.00**	8.478	1.588	10.066	23.00	**4.00**	**4.00**
Yang et al. [17]	62.50	4.808	**0.034**	**4.843**	16.11	10.56	10.83	62.00	**4.805**	**0.031**	**4.837**	18.00	9.00	11.00
GA-DDPG [48] hold	55.00	7.145	0.129	7.274	**8.61**	17.78	18.61	50.00	7.305	0.135	7.440	**5.00**	23.00	22.00
GA-DDPG [48] w/o hold	28.33	**4.747**	0.133	4.881	9.17	34.44	28.06	33.00	4.948	0.123	5.071	10.00	33.00	24.00

TABLE II: Performance of the baselines with our adopted metrics (Sec. IV) on the four evaluation setups.

assume ground-truth object pose, we bypass grasp generation and directly use the pre-generated grasps as in the OMG Planner for the task planning step.

- **GA-DDPG [48].** This is a neural network policy trained with RL for grasping static objects. It takes in a segmented point cloud of the target object and directly outputs the robot's target joint position. The policy is closed-loop as the network is ran every 0.15 seconds. To obtain the input, we render a point cloud from a wrist-mounted camera following [48] and segment the point cloud using the ground-truth segmentation mask. Once the gripper reaches the object, we switch to the same hand coded policy as in the OMG Planner. We use the model trained in [48]. Since it is trained only for grasping static objects, we evaluate this baseline with two variants: holding still until the human hand comes to a stop as in the OMG Planner ("hold") and without any hold ("w/o hold").

We note that none of these baselines has been trained on the benchmark. Our aim is to first provide the results and analysis of existing approaches and models. With proper baselines, our benchmark can pave the way for future handover systems benefited from training in the environment.

Results. Tab. II shows the results on the test splits of the four setups (i.e., S0, S1, S2, and S3). Below we focus the discussion on S0 (default), since the results on the other three setups also show similar trends.

We see that the OMG Planner achieves competitive success rate (62.50%) among all the baselines. Besides, the failure cases are dominated by robot-human contact (27.28%). This is unsurprising since the planner takes no account of the hand's position and thus might generate hand-colliding trajectories. However, object dropping (8.33%) and timeout (1.39%) both achieve the lowest occurrence rate among all the baselines. This suggests that with accurate object pose estimates and robust grasp generation, motion planning based approaches can be very reliable. Despite the high efficacy, it falls short on efficiency—the OMG Planner achieves the highest mean accumulated time among all the baselines on both execution (8.309s) and planning (1.414s). The first two rows in Fig. 4 shows qualitative examples of a success (top) and a failure due to robot-human contact (bottom).

Yang et al. achieves a comparable success rate to the OMG Planner (64.58% versus 62.50%). Yet the occurrence rate of robot-human contact is significantly lower (17.36% versus 27.78%). This is attributed to the system's tendency of approaching the object directly from the front side, which is typically free from collision with the hand that holds the object from the opposite side. Since the system is tailored for reactive handovers, the robot is moving with higher acceleration and deceleration. This causes the object to drop more easily during contact, resulting in a higher failure rate of "drop" (11.81% versus 8.33%). However, the higher peak speed also improves the efficiency. The system achieves competitive mean accumulated time on execution (4.864s), only behind the "w/o hold" variant of GA-DDPG. The middle two rows in Fig. 4 shows qualitative examples of a success (top) and a failure due to object dropping (bottom).

GA-DDPG (hold) achieves a lower success rate compared to the OMG Planner and Yang et al. (50.00% versus 62.50% and 64.58%). This is due to the more ambiguous point cloud input compared to ground-truth object pose and pre-generated grasps. We also see a much higher rate on timeout (e.g., 25.69% versus 1.39%), many of which are resulted from grasping in wrong locations. In contrast, the failure rate due to contacting human is much lower (e.g., 4.86% versus 27.78%), since mis-grasps often happen even before the gripper gets close enough to the hand. In terms of efficiency, the execution time is comparable to Yang et al. (4.664 versus 4.864 seconds), but planning is slightly slower (0.142 versus 0.036 seconds) due to additional point cloud processing.

Finally, GA-DDPG (w/o hold) achieves the lowest success rate among all the baselines (36.81%). The failures are often caused by the gripper contacting the human hand or object when the hand and object are still actively moving, since the policy was never trained to adapt to moving objects. However, this baseline achieves the lowest mean accumulated time on execution and total, since it is not forced to hold. The last two rows in Fig. 4 shows qualitative examples of a success (top) and a failure from knocking down the object (bottom) from GA-DDPG (w/o hold).

Correlation with Real-World Evaluation. A critical question for a simulation benchmark is whether the achieved

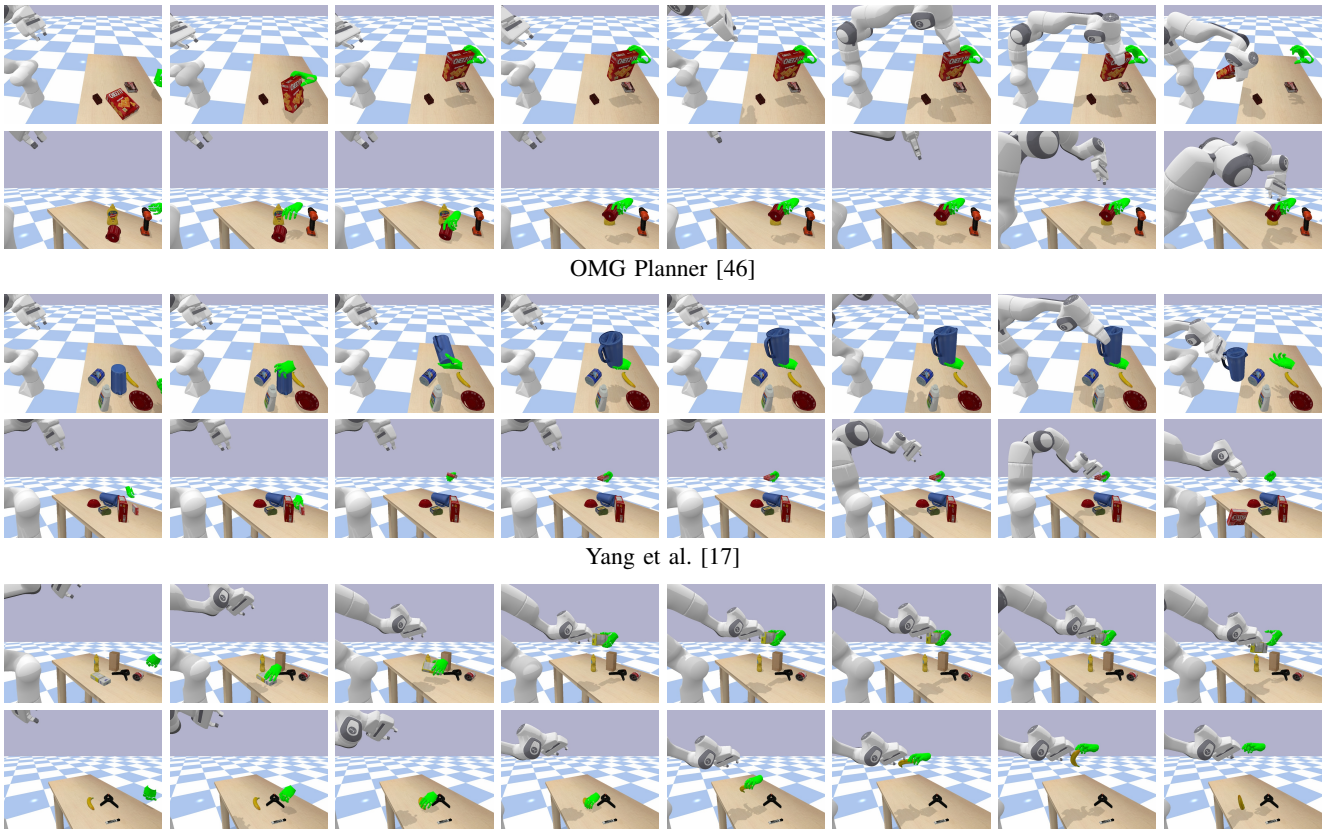


Fig. 4: Qualitative results of handovers. For each baseline, we show one success (top) and one failure (bottom) case.

performance translates into real-world performance. Below we refer to a relevant real-world user study reported in Sec. 4.3 of [48]. The study compares Yang et al. [17] and GA-DDPG [48] on H2R handover with 6 participants. We excerpt the results in Tab. III.

We observe a positive correlation between the performance in the real world and on HandoverSim. In terms of the success rate, Yang et al. has a slight edge over GA-DDPG in Tab. III (i.e., 82% versus 80%), and the same trend also holds on HandoverSim (e.g., 62.78% versus 55.00% on S1). In terms of efficiency, Yang et al. achieves a lower approach time than GA-DDPG in Tab. III (i.e., 10.7 versus 12.7 seconds), which again holds for the mean accumulated time on HandoverSim (e.g., 4.758 versus 6.927 seconds).

In a subjective evaluation (Fig. 5 (bottom) in [48]), the users are asked to score each given statement from 1 (strongly disagree) to 5 (strongly agree). The scores for the statement *"The robot and I worked fluently as a team to transfer objects."* for GA-DDPG are (4, 4, 4, 4, 4, 3), while the scores for Yang et al. are (5, 5, 4, 4, 4, 3) (Fig. 10 in [17]). The higher average score of Yang et al. (i.e., 4.17 versus 3.83) also positively correlates with its better efficiency performance on HandoverSim.

Despite the correlation, we also see an offset between the performance in real and simulation. On one hand, the success rates in real are constantly higher than on HandoverSim (e.g., for GA-DDPG, 80% versus 55.00% on S1). This is because real users are often cooperative and can help adjust the pose of the object to prevent grasping failures, making the system more error tolerant. On the other hand, the efficiency performance in real is constantly lower than on HandoverSim (e.g., for Yang et al., a 10.7 seconds approach time versus a 4.758 seconds accumulated time on S1). This offset can be attributed to two factors. First, the reported time on HandoverSim does not contain any latency from perception, since the baselines directly consume the ground-truth state information. In contrast, the real world systems involve perception stacks (e.g., human body tracking and hand segmentation in [17]). Second, [17] uses an extra low level control module (Riemannian Motion Policies) to achieve smooth motion. This adds additional latency to the loop. In constrast, HandoverSim uses a simple PD controller without any sophisticated control modules.

	avg. success rate (%)	avg. approach time (s)
Yang et al. [17]	**82**	**10.7**
GA-DDPG [48]	80	12.1

TABLE III: Results of the real-world user study from [48].

VI. Conclusions

We have introduced a new simulation benchmark for H2R handovers. We have analyzed the performance of a set of baselines on our benchmark, and validated its credibility by showing a correlation with a real-world user study.

REFERENCES

[1] V. Ortenzi, A. Cosgun, T. Pardi, W. P. Chan, E. Croft, and D. Kulić, "Object handovers: A review for robotics," *T-RO*, vol. 37, no. 6, pp. 1855–1873, 2021.

[2] T.-Y. Lin, M. Maire, S. Belongie, J. Hays, P. Perona, D. Ramanan, P. Dollár, and C. L. Zitnick, "Microsoft COCO: Common Objects in Context," in *ECCV*, 2014.

[3] O. Russakovsky, J. Deng, H. Su, J. Krause, S. Satheesh, S. Ma, Z. Huang, A. Karpathy, A. Khosla, M. Bernstein, A. C. Berg, and L. Fei-Fei, "ImageNet Large Scale Visual Recognition Challenge," *IJCV*, vol. 115, no. 3, pp. 211–252, 2015.

[4] L. Fan, Y. Zhu, J. Zhu, Z. Liu, O. Zeng, A. Gupta, J. Creus-Costa, S. Savarese, and L. Fei-Fei, "SURREAL: Open-source reinforcement learning framework and robot manipulation benchmark," in *CoRL*, 2018.

[5] M. Savva, A. Kadian, O. Maksymets, Y. Zhao, E. Wijmans, B. Jain, J. Straub, J. Liu, V. Koltun, J. Malik, D. Parikh, and D. Batra, "Habitat: A platform for embodied AI research," in *ICCV*, 2019.

[6] T. Yu, D. Quillen, Z. He, R. Julian, K. Hausman, C. Finn, and S. Levine, "Meta-World: A benchmark and evaluation for multi-task and meta reinforcement learning," in *CoRL*, 2019.

[7] F. Xia, W. B. Shen, C. Li, P. Kasimbeg, M. E. Tchapmi, A. Toshev, R. Martín-Martín, and S. Savarese, "Interactive Gibson Benchmark: A benchmark for interactive navigation in cluttered environments," *RA-L*, vol. 5, no. 2, pp. 713–720, 2020.

[8] S. James, Z. Ma, D. R. Arrojo, and A. J. Davison, "RLBench: The robot learning benchmark & learning environment," *RA-L*, vol. 5, no. 2, pp. 3019–3026, 2020.

[9] A. Clegg, Z. Erickson, P. Grady, G. Turk, C. C. Kemp, and C. K. Liu, "Learning to collaborate from simulation for robot-assisted dressing," *RA-L*, vol. 5, no. 2, pp. 2746–2753, 2020.

[10] Z. Erickson, V. Gangaram, A. Kapusta, C. K. Liu, and C. C. Kemp, "Assistive Gym: A physics simulation framework for assistive robotics," in *ICRA*, 2020.

[11] F. Xiang, Y. Qin, K. Mo, Y. Xia, H. Zhu, F. Liu, M. Liu, H. Jiang, Y. Yuan, H. Wang, L. Yi, A. X. Chang, L. J. Guibas, and H. Su, "SAPIEN: A SimulAted Part-based Interactive ENvironment," in *CVPR*, 2020.

[12] M. Deitke, W. Han, A. Herrasti, A. Kembhavi, E. Kolve, R. Mottaghi, J. Salvador, D. Schwenk, E. VanderBilt, M. Wallingford, L. Weihs, M. Yatskar, and A. Farhadi, "RoboTHOR: An open simulation-to-real embodied AI platform," in *CVPR*, 2020.

[13] X. Lin, Y. Wang, J. Olkin, and D. Held, "SoftGym: Benchmarking deep reinforcement learning for deformable object manipulation," in *CoRL*, 2020.

[14] Y. Lee, E. S. Hu, and J. J. Lim, "IKEA furniture assembly environment for long-horizon complex manipulation tasks," in *ICRA*, 2021.

[15] Y.-W. Chao, W. Yang, Y. Xiang, P. Molchanov, A. Handa, J. Tremblay, Y. S. Narang, K. Van Wyk, U. Iqbal, S. Birchfield, J. Kautz, and D. Fox, "DexYCB: A benchmark for capturing hand grasping of objects," in *CVPR*, 2021.

[16] R. Newbury, A. Cosgun, T. Crowley-Davis, W. P. Chan, T. Drummond, and E. Croft, "Visualizing robot intent for object handovers with augmented reality," *arXiv preprint arXiv:2103.04055*, 2021.

[17] W. Yang, C. Paxton, A. Mousavian, Y.-W. Chao, M. Cakmak, and D. Fox, "Reactive human-to-robot handovers of arbitrary objects," in *ICRA*, 2021.

[18] W. Yang, C. Paxton, M. Cakmak, and D. Fox, "Human grasp classification for reactive human-to-robot handovers," in *IROS*, 2020.

[19] P. Rosenberger, A. Cosgun, R. Newbury, J. Kwan, V. Ortenzi, P. Corke, and M. Grafinger, "Object-independent human-to-robot handovers using real time robotic vision," *RA-L*, vol. 6, no. 1, pp. 17–23, 2021.

[20] H. Nemlekar, D. Dutia, and Z. Li, "Object transfer point estimation for fluent human-robot handovers," in *ICRA*, 2019.

[21] P. Ardón, M. E. Cabrera, È. Pairet, R. P. A. Petrick, S. Ramamoorthy, K. S. Lohan, and M. Cakmak, "Affordance-aware handovers with human arm mobility constraints," *RA-L*, vol. 6, no. 2, pp. 3136–3143, 2021.

[22] P. Basili, M. Huber, T. Brandt, S. Hirche, and S. Glasauer, *Investigating Human-Human Approach and Hand-Over*, 2009, pp. 151–160.

[23] A. Mason and C. L. MacKenzie, "Grip forces when passing an object to a partner," *Experimental Brain Research*, vol. 163, no. 2, pp. 173–187, 2005.

[24] A. G. Eguíluz, I. Rañó, S. A. Coleman, and T. M. McGinnity, "Reliable object handover through tactile force sensing and effort control in the shadow robot hand," in *ICRA*, 2017.

[25] M. Savva, A. X. Chang, A. Dosovitskiy, T. Funkhouser, and V. Koltun, "MINOS: Multimodal indoor simulator for navigation in complex environments," *arXiv preprint arXiv:1712.03931*, 2017.

[26] E. Kolve, R. Mottaghi, W. Han, E. VanderBilt, L. Weihs, A. Herrasti, D. Gordon, Y. Zhu, A. Gupta, and A. Farhadi, "AI2-THOR: An Interactive 3D Environment for Visual AI," *arXiv preprint arXiv:1712.05474*, 2017.

[27] Y. Wu, Y. Wu, G. Gkioxari, and Y. Tian, "Building generalizable agents with a realistic and rich 3D environment," *arXiv preprint arXiv:1801.02209*, 2018.

[28] C. Yan, D. Misra, A. Bennnett, A. Walsman, Y. Bisk, and Y. Artzi, "CHALET: Cornell House Agent Learning Environment," *arXiv preprint arXiv:1801.07357*, 2018.

[29] A. Das, S. Datta, G. Gkioxari, S. Lee, D. Parikh, and D. Batra, "Embodied question answering," in *CVPR*, 2018.

[30] F. Xia, A. R. Zamir, Z. He, A. Sax, J. Malik, and S. Savarese, "Gibson Env: Real-world perception for embodied agents," in *CVPR*, 2018.

[31] K. Ehsani, W. Han, A. Herrasti, E. VanderBilt, L. Weihs, E. Kolve, A. Kembhavi, and R. Mottaghi, "ManipulaTHOR: A framework for visual object manipulation," in *CVPR*, 2021.

[32] X. Puig, T. Shu, S. Li, Z. Wang, Y.-H. Liao, J. B. Tenenbaum, S. Fidler, and A. Torralba, "Watch-And-Help: A challenge for social perception and human-AI collaboration," in *ICLR*, 2021.

[33] X. Puig, K. Ra, M. Boben, J. Li, T. Wang, S. Fidler, and A. Torralba, "VirtualHome: Simulating household activities via programs," in *CVPR*, 2018.

[34] R. Ye, W. Xu, Z. Xue, T. Tang, Y. Wang, and C. Lu, "H2O: A benchmark for visual human-human object handover analysis," in *ICCV*, 2021.

[35] R. Sanchez-Matilla, K. Chatzilygeroudis, A. Modas, N. F. Duarte, A. Xompero, P. Frossard, A. Billard, and A. Cavallaro, "Benchmark for human-to-robot handovers of unseen containers with unknown filling," *RA-L*, vol. 5, no. 2, pp. 1642–1649, 2020.

[36] Y. Xiang, T. Schmidt, V. Narayanan, and D. Fox, "PoseCNN: A convolutional neural network for 6D object pose estimation in cluttered scenes," in *RSS*, 2018.

[37] E. Coumans and Y. Bai, "PyBullet: a Python module for physics simulation for games, robotics and machine learning," https://pybullet.org, 2016–2021.

[38] V. Makoviychuk, L. Wawrzyniak, Y. Guo, M. Lu, K. Storey, M. Macklin, D. Hoeller, N. Rudin, A. Allshire, A. Handa, and G. State, "Isaac Gym: High performance gpu-based physics simulation for robot learning," *arXiv preprint arXiv:2108.10470*, 2021.

[39] J. Romero, D. Tzionas, and M. J. Black, "Embodied hands: Modeling and capturing hands and bodies together," in *SIGGRAPH Asia*, 2017.

[40] I. Kalevatykh, "mano_pybullet: MANO-based hand models for the PyBullet simulator," https://github.com/ikalevatykh/mano_pybullet, 2020.

[41] X. B. Peng, E. Coumans, T. Zhang, T.-W. Lee, J. Tan, and S. Levine, "Learning agile robotic locomotion skills by imitating animals," in *RSS*, 2020.

[42] A. Rajeswaran, V. Kumar, A. Gupta, G. Vezzani, J. Schulman, E. Todorov, and S. Levine, "Learning complex dexterous manipulation with deep reinforcement learning and demonstrations," in *RSS*, 2018.

[43] OpenAI, M. Andrychowicz, B. Baker, M. Chociej, R. Józefowicz, B. McGrew, J. Pachocki, A. Petron, M. Plappert, G. Powell, A. Ray, J. Schneider, S. Sidor, J. Tobin, P. Welinder, L. Weng, and W. Zaremba, "Learning dexterous in-hand manipulation," *arXiv preprint arXiv:1808.00177*, 2018.

[44] A. Nagabandi, K. Konolige, S. Levine, and V. Kumar, "Deep dynamics models for learning dexterous manipulation," in *CoRL*, 2019.

[45] G. Brockman, V. Cheung, L. Pettersson, J. Schneider, J. Schulman, J. Tang, and W. Zaremba, "OpenAI Gym," *arXiv preprint arXiv:1606.01540*, 2016.

[46] L. Wang, Y. Xiang, and D. Fox, "Manipulation trajectory optimization with online grasp synthesis and selection," in *RSS*, 2020.

[47] C. Eppner, A. Mousavian, and D. Fox, "A billion ways to grasps: An evaluation of grasp sampling schemes on a dense, physics-based grasp data set," in *ISRR*, 2019.

[48] L. Wang, Y. Xiang, W. Yang, A. Mousavian, and D. Fox, "Goal-auxiliary actor-critic for 6D robotic grasping with point clouds," in *CoRL*, 2021.